PERGAMON

Vision Research 39 (1999) 149–157

Vision Research

# Residual vision in the blind field of hemidecorticated humans predicted by a diffusion scatter model and selective spectral absorption of the human eye

Jocelyn Faubert [a,*], Vasile Diaconu [a], Maurice Ptito [b,c], Alain Ptito [c]

[a] *École d'optométrie, Université de Montréal, CP 6128, Succursalle Centre-Ville, Montréal, Québec H3C 3J7, Canada*
[b] *Département de Psychologie, Université de Montréal, Montréal, Canada*
[c] *Montreal Neurological Institute, McGill University, Montreal, Canada*

Received 13 February 1997; received in revised form 16 February 1998

**Abstract**

The notion of blindsight was recently challenged by evidence that patients with occipital damage and contralateral field defects show residual islands of vision which may be associated with spared neural tissue. However, this possibility could not explain why patients who underwent the resection or disconnection of an entire cerebral hemisphere exhibit some forms of blindsight. We present here a model for the detection of intraocular scatter, which can account for human sensitivity values obtained in the blind field of hemidecorticated patients. The model demonstrates that, under controlled experimental conditions i.e. where the extraocular scatter is eliminated, Lambertian intraocular scatter alone can account for the visual sensitivities reported in these patients. The model also shows that it is possible to obtain a sensitivity in the blind field almost equivalent to that in the good field using the appropriate parameters. Finally, we show with in-vivo spectroreflectometry measurements made in the eyes of our hemidecorticated patients, that the relative drop in middle wavelength sensitivity generally obtained in the blind field of these patients can be explained by selective intraocular spectral absorption. 

*Keywords:* Blindsight; Residual vision; Scatter; Eye; Spectroreflectometry; Spectral sensitivity; Luminance threshold; Consciousness

## 1. Introduction

For the past two decades there has been substantial evidence that patients whose primary visual cortex has been destroyed or deafferented by vascular, traumatic, or neoplastic lesions can demonstrate a variety of residual visual functions in the corresponding homonymous hemianopic visual field (Weiskrantz, 1986; Stoerig & Cowey, 1995). These findings have recently been challenged by evidence that the hemianopic field determined by standard perimetry may in fact still have residual islands of visual function when using a retinal image stabilizing procedure (Fendrich, Wessinger & Gazzaniga, 1992). Furthermore, using magnetic resonance imaging, these researchers identified spared cortical tissue in the damaged hemisphere which could be the source of the small islands of vision obtained within the scotomatous visual field. Blindsight has also been challenged earlier by Campion and coworkers (Campion, Latto & Smith, 1983) where they suggested that blindsight could be the result of either scattered light, near-threshold vision, or spared cortex. However, the latter suggestion, along with the Fendrich et al.'s results, cannot explain the residual vision observed in the blind field of patients in whom the whole cerebral hemisphere has been removed or deafferanted (Perenin & Jeannerod, 1978; Ptito, Lassonde, Leporé & Ptito, 1987; Perenin, 1991; Ptito, Leporé, Ptito & Lassonde, 1991). In a recent paper, we have proposed that intraocular diffusion and scatter are the probable sources of residual visual functions, i.e. spectral sentivity (Stoerig, Faubert, Pito, Diaconu & Ptito, 1996). We extrapolated further that, under photopic conditions, the most common site of light detection as a result of scatter must be the central visual field area (CVFA) for a target positioned in the blind field, and we also suggested that spectral absorption in the eye must be considered

* Corresponding author. E-mail: faubert@ere.umontreal.ca

0042-6989/98/$ - see front matter 
PII: S0042-6989(98)00107-2

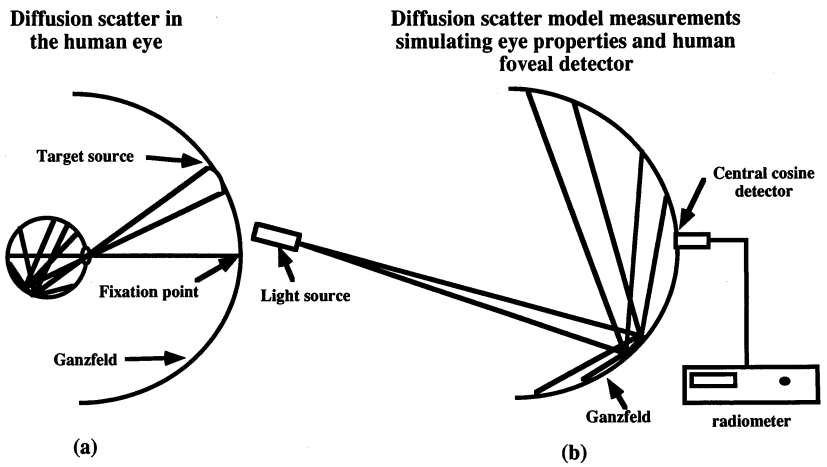


Fig. 1. Simplified schematic representation of the eye facing a Ganzfeld (Fig. 1a) and the mechanical scatter diffusion model (Fig. 1b). A cosine detector was placed in the center of the model retina (Ganzfeld) and was interfaced with a radiometer. Stimuli were projected in different areas of the Ganzfeld for different target sizes. The amount of energy measured by the radiometer was taken as the sensitivity value of the model.

(Faubert, Diaconu, Ptito & Ptito, 1995). In studies on residual vision in hemicorticectomized patients, some experimenters were mainly concerned with extraocular scatter (King, Azzopardi, Cowey, Oxbury & Oxbury, 1996), but we believe this control to be insufficient. One reason is that scatter within the eye must generally be more significant than scatter outside of it because the eye is a miniature reflective chamber. In this paper, we present a model composed of mechanical and electronic parts in an attempt to simulate light scatter properties. We shall furthermore determine whether such a model can explain the visual sensitivity results obtained in the blind hemifield of hemidecorticated patients. Finally, the model is extended to include a mathematical representation of the absorption and reflective properties of the retinal layers (Appendix A) to explain the relative decrease of sensitivity observed in the blind field of hemidecorticated patients.

### *1.1. Model assumptions*

There are three main assumptions which were made prior to developing the model. First, in the human eye there is an important source of Lambertian (diffuse) scatter and not just specular reflection (LeGrand, 1958). Specular reflection corresponds to the light which is reflected directly with 'mirror-like' properties. The direction of this scatter can be established by determining the geometry of the incident light. This is analogous to pointing a flashlight directly at a mirror and being blinded by this reflected light because it bounces right back towards the original light source. Furthermore, although specular reflection is a well known and important scatter source in the eye (LeGrand, 1958), Lambertian or diffuse reflection is also in intraocular scatter. If the internal surface of the eye primarily generates specular reflections, it would be impossible to detect the retinal structures which are readily observed with an ophthalmoscope and only reflected lights would be seen.

Second, we assume that under photopic conditions the CVFA is the region with the best sensitivity and therefore the probable locus for diffusion scatter detection. This CVFA advantage is a well known fact and is referred to as the 'island of vision' (Hood & Finkelstein, 1986). Therefore, if diffusion scatter were to play a role in residual vision, it should be most easily detected by the observer in the CVFA for photopic conditions. As will be clarified later, this is not to say that other retinal locations will not respond to scatter. In fact if a stimulus is positioned within 10° of eccentricity from the vertical midline many retinal locations along the vertical axis may respond to the light stimulus. This point will be demonstrated with our patient and model results below. Furthermore, this model relates to luminance detection under controlled conditions because clearly, any portion of the retina can potentially respond to the scatter emanating from stimuli presented at suprathreshold luminance levels.

The third assumption is that given that the eye is spherical, a Ganzfeld environment is a good model to assess the role of intraocular Lambertian scatter and its role in residual vision. In fact, an open-ended Ganzfeld field, such as the one used in this study, is even a better means to isolate the primary Lambertian scatter because the specular reflection and the integrative energy scatter is not captured at the CVFA detector site.

## 2. Methods

### *2.1. Apparatus and procedure*

Fig. 1 illustrates the model in which a Ganzfeld field

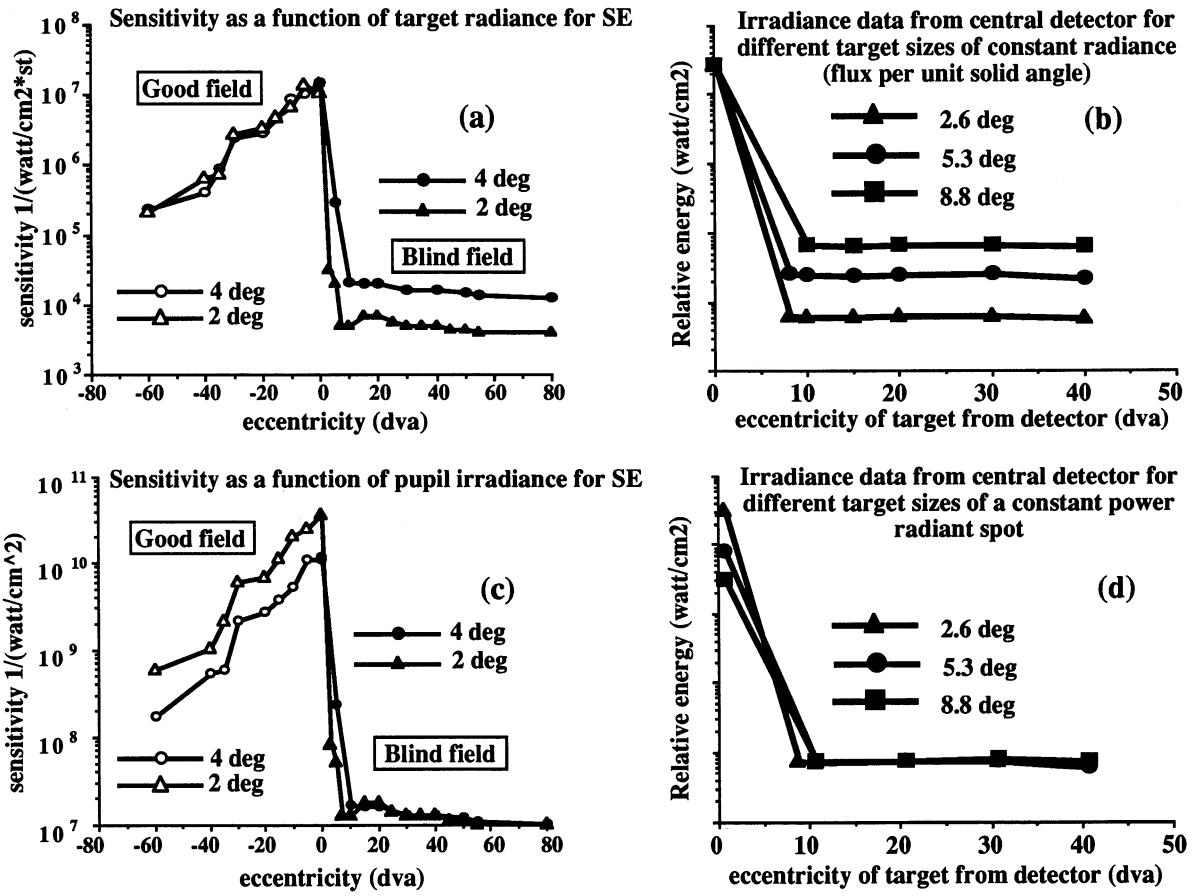


Fig. 2. Sensitivity as a function of eccentricity in the good and blind field of partially hemidecorticated patient SE ((Fig. 2a), adapted from (Stoerig et al., 1996) and for the model (Fig. 2b). Two target sizes were evaluated for SE and three target sizes for the model. The data in (Fig. 2a) represent sensitivity values computed from target radiance. Fig. 2b illustrates the model data obtained from the central detector for different targets of constant radiance (same flux per unit solid angle). The same data are represented for the patient in (Fig. 2c) where the sensitivity values are computed from pupil irradiance. This corresponds to the relative total energy required to obtain a threshold for a given testing condition. The total energy representation for the model (when the size of the target is factored in) is presented in (Fig. 2d). This corresponds to the model data obtained for different target sizes generated from a constant power radiant spot. Note that the model data corresponds with the data obtained in the blind field of SE.

was used to simulate the internal human eye. This is an obvious oversimplification of the scatter properties of the eye as a whole given that we didn't take into consideration the scatter generated from the optics of the eye. Nevertheless, the model does allow us to simulate and isolate the role of diffusion scatter properties.

We cut a hole in the center of the Ganzfeld and placed an integrative cosine detector to act as our CVFA receptors. In this way we could project a stimulus at different locations in the Ganzfeld and directly measure the energy level at the detector site. The amount of energy measured by the radiometer (Optronic Spectroradiometer model 736) receiving its input from the cosine detector is the sensitivity measure for the system. The measures obtained with the present model were compared with our patient data previously reported (Stoerig et al., 1996). Essentially, these data were obtained under conditions where the entire visual field was adapted with a 45cd/m$^2$ white background, and the light source was generated from behind the adaptive surface while the size of the target was controlled by an aperture. This was done to avoid producing scatter within the adaptive field itself.

## 3. Results

One of the typical responses obtained when testing the blind visual field of our hemidecorticated patients is represented in Fig. 2a. The data were plotted on an energy scale as opposed to a luminance scale so that it becomes possible to directly compare them with the model data (Fig. 2b).

Within the patient's blind field there is a sharp drop-off of sensitivity from the fovea to about 10° of retinal eccentricity where it then stabilizes for a given target size. This is observed in the right portion of Fig. 2a (fixation represented as the zero point on the x-axis). This is in sharp contrast with the good visual field where there is a continual sensitivity drop with increasing eccentricity (left portion of Fig. 2a) which is expected for a normal observer. Fig. 2b demonstrates that the data obtained with the model setup are very similar to the blind hemifield data of our hemidecorticated patients with regards to the shape of the functions. There is a sharp drop-off up to 10° eccentricity and then the sensitivity of the model remains constant with increasing eccentricity.

There appears to be spatial summation (better sensitivity with increasing target size) in the blind field of the patients for relatively large target sizes (Fig. 2a right) which is also present in the model data (Fig. 2b). In a normal visual system, and under similar experimental conditions used to test our patients (400 ms and 1° target sizes or greater), there is no spatial summation since these conditions are beyond Ricco's area (Hood & Finkelstein, 1986). As argued in the next paragraph, the spatial summation effect in the blind field is observed because the data are represented as relative density measures (e.g. cd/m$^2$). In the light of the scatter hypothesis, the data must be analyzed in terms of the total energy entering the eye.

In Fig. 2c, we have replotted the patient's data from physical measurements made at the level of the pupil. This allowed us to measure the relative change in total energy entering the eye for the data presented in Fig. 2a. Fig. 2c shows that we now have two overlapping functions for the two different target sizes in the blind hemifield, whereas the good field shows spatial summation (Fig. 2c). When we factor in the target size to represent the total energy generated by the various target sizes for a given model threshold, we obtain overlapping functions (Fig. 2d) just like the blind field data of the patient shown in Fig. 2c.

## 4. Discussion

The present data suggest that the sensitivity profiles obtained in the blind field of hemidecorticated patients may be accounted for by Lambertian diffusion scatter properties of the eye. The simple model presented above is in itself sufficient to explain the results obtained with our hemidecorticated patients. It is important to note that, even under well controlled conditions which eliminate extraocular scatter, it is possible to obtain sensitivity values in the blind field of hemidecorticated patients solely on the basis of diffusion scatter within the eye. Whether one obtains a sensitivity value or not depends on the size of the stimulus. For instance, if the stimulus target size used is 5° in diameter, it may require a luminance difference of 3 log units between the good and blind field to obtain thresholds but if a target size of 10° is used then it may require half that amount in relative difference. This occurs because changing the size of a given target also modifies the total energy entering the eye and as a consequence less energy is required to produce the same stimulation for a given unit of area.

In essence, it appears that the sensitivity measures obtained in the good and blind fields function on two different mechanisms. The good visual field functions according to the amount of energy for a given area; the residual vision in the blind field depends upon the total amount of energy entering the eye because the CVFA receptors detect the energy which has been scattered from its original site of projection. The present model is consistent with the fact that we could not change the sensitivity in the blind field of patients when we modify only a local adapting background whereas the sensitivity values change in a normal fashion when the entire visual field is adapted (Stoerig et al., 1996). What we show here is that the sensitivity in the blind field was probably obtained from CVFA receptors.

### 4.1. Additional control experiments

In addition to the patient data reported in the previous study (Stoerig et al., 1996), we have tested the same three hemidecorticated patients described in that paper (DR, JB and SE) for spatial summation at a fixed eccentricity (20°) and the data are shown in Fig. 3a. The results are consistent with the previous data for patient SE shown in Fig. 2a and in line with our 'diffusion scatter-CVFA detection' model. The ordinate represents sensitivity on a relative density scale and what can be observed is that the sensitivity in the good field for four different target sizes (2, 4, 8, 12°) remains constant while there appears to be spatial summation in the blind field.

In the previous paper (Stoerig et al., 1996) we also reported a control condition for patient SE where we estimated the effect of different configurations of background intensity on a differential luminance threshold. In one condition (local condition) we adapted a small area on which we superimposed the target to obtain thresholds. In another condition (global condition), we adapted the entire visual field and assessed the effect on thresholds for different background intensity levels. The assumption was that if the detection was really local, as assumed by the residual vision hypothesis, there should be no difference between the local and global adapting conditions. On the other hand, if the diffusion scatter model is correct, there should be a difference between the global and local conditions. Those results clearly

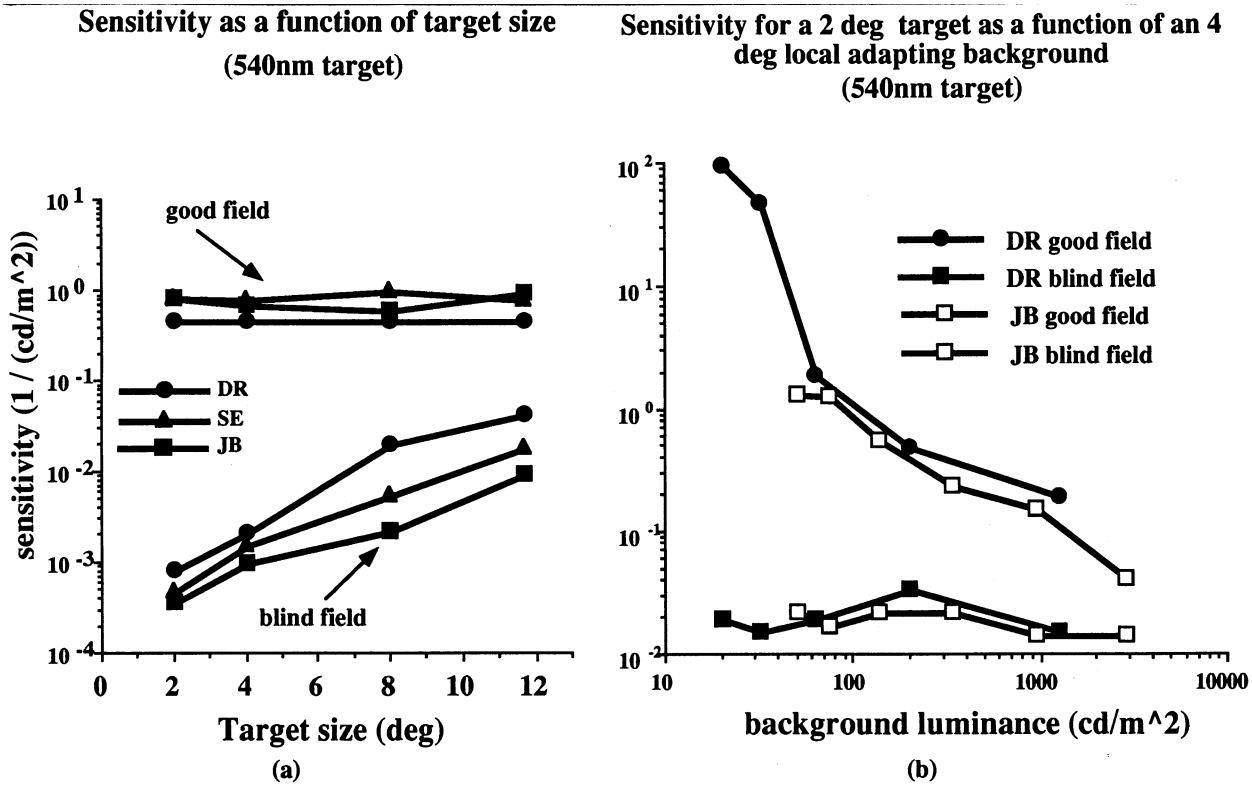


Fig. 3. Spatial summation data obtained at 20° eccentricity in the blind and good fields of three hemidecorticated (DR, SE, and JB) patients (Fig. 3a). The good field data show flat functions as expected when target sizes are beyond Ricco's area of spatial summation. Data from the blind field show what wrongly appears to be spatial summation in the blind field. See text for details. Fig. 3b shows sensitivity values obtained in the good and blind fields of two patients (DR and JB) for a 2° target superimposed on a 4° local adapted background of different intensities. Note that the good field data show the expected decreased sensitivity with increasing background intensity while the blind field data show flat functions implying that the detection of the target was in fact occuring somewhere else in the visual field.

showed that in the good field, the effect of local and global backgrounds were the same on the detection thresholds implying that the sensitivity in the good field was truly obtained from the target position area. The results from the blind field show a similar response curve as the good field when the entire background was adapted. However, the thresholds obtained in the local condition show no changes with local background intensity changes even at very high luminance levels. We tested the 'local' background condition in the good and blind field of subjects DR and JB for a range of luminances, and the data are shown in Fig. 3b. Essentially, the data replicate our previous study and show that the detection of the target was not occuring at the tested site as predicted by our 'diffusion scatter-CVFA detection' model.

### 4.2. Testing under scotopic conditions

Because some testing of hemidecorticated patients has been carried out under scotopic conditions it is worth considering how measurements undertaken in such conditions may differ from those obtained under photopic conditions in relation to light scatter. First of all, it must be obvious to the reader at this point that testing for blindsight under scotopic conditions is not a very good idea for a number of reasons. The main reason is that the remaining functional visual field locations, other than the testing site, are not light adapted which makes these locations all the more sensitive to any form of scattered light including specular reflections and Lambertian scatter. It becomes very difficult under these circumstances to predict where the detection of scattered light may occur. However, it is possible to speculate that, under scotopic adaptation conditions, a possible site for detection of scattered light would not only be the CVFA where there is a unique concentration of cones but, rather, the site would probably be a semicircular ring where there is a higher density of rods (between 15–20°). Of course, if the stimuli are presented under suprathreshold light detection conditions then scatter detection could be obtained from almost any area of the visual field which remains functional.

### 4.3. Selective spectral absorption

There was one particular result obtained in our previous study which the model could not explain. When we

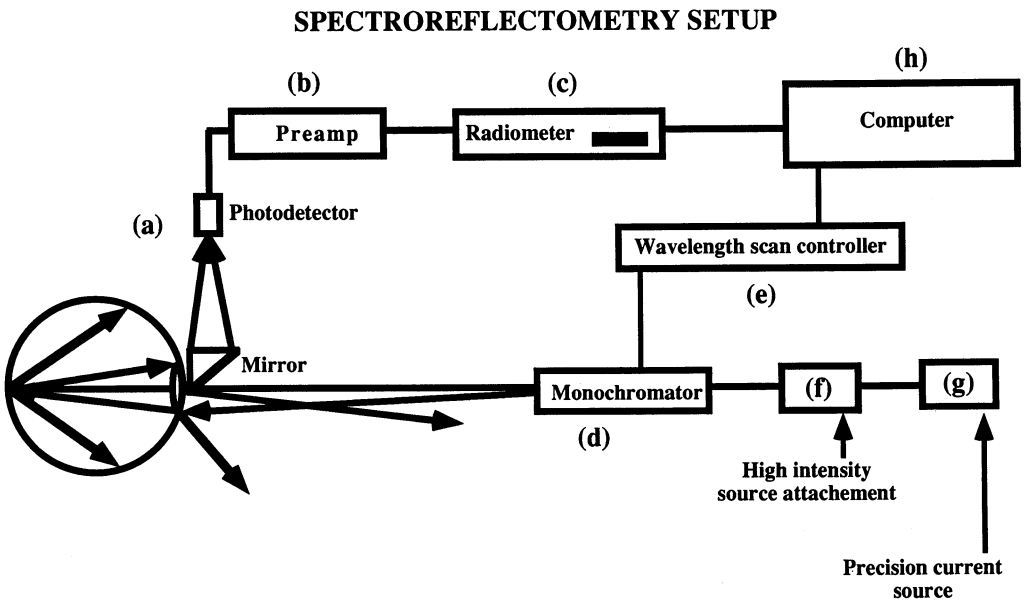


Fig. 4. Schematic representation of the spectroradiometric setup used to make spectroreflectometry measurements in the eyes of two hemidecorticated patients (DR and SE). The setup is composed of a silicon photodetector (Fig. 4a), a preamplificator (Fig. 4b), a spectroradiometer (Fig. 4c), a monochromator (Fig. 4d), a wavelength scan controler model (Fig. 4e), a high intensity source (Fig. 4f), a precision current source (Fig. 4fg), and a computer interface (Fig. 4h). The subjects' pupils were dilated and the measurements were made at 20° eccentricity. Wavelengths bewteen 400 and 660 nm were assessed in 10 nm steps. The light source entered the eye through half the pupil and the light exiting from the other half was redirected onto the photodetector by a small diagonal mirror.

tested for spectral sensitivity functions under photopic conditions, we obtained a relative decrease in sensitivity for the middle wavelength region of the visible spectrum (Stoerig et al., 1996). One possibility consistent with the present model is that the energy not reflected back to the CVFA was absorbed by the tissues of the eye. We tested this assumption by making spectroreflectometry measurements (Rushton, 1962) in the eyes of patients DR and SE in order to determine if selective wavelength absorption of the eye could account for the relative decrease of sensitivity in the middle wavelength region of the spectrum (Faubert et al., 1995).

Spectroreflectometry measurements are defined here as the energy measured at the pupil exit when the eye is presented with a given light source. It is possible to establish what part of the visible spectrum was absorbed by the eye when it is presented with a light source by measuring the amount of energy entering and leaving the eye while taking into account the energy which is absorbed by the optics (Wyszecki & Stiles, 1982).

Fig. 4 illustrates a schematic of the apparatus used for the spectroreflectometry measurements. The setup is composed of a light source entering the eye in half the pupil. Over the other half of the pupil, there is a small 45° mirror which directs the light coming out of the pupil onto a light detector. The spectroreflectometry system was composed of: an Optronic Spectroradiometer model 736; a monochromator model 746-D; a wavelength scan controller model 740-1C1D; a preamplificator model 736; a precision current source model 65DS; a silicon photodetector; and a computer interface. Wavelengths from 400 to 660 nm in 10 nm steps were evaluated. The pupil of the subject was dilated with cyclogil (topical) at least half an hour before testing.

Fig. 5a illustrates the relative difference in spectral sensitivity between the good and blind fields as a good/blind field ratio for each wavelength tested and Fig. 5b shows the spectroreflectometry measurements obtained for these same two subjects. The results clearly show that the region of the visible spectrum, where patients demonstrate a selective reduction of sensitivity in the blind field relative to the good field, consists of the same wavelengths which are most absorbed by the eye. What is absorbed by the eye cannot be scattered, and what is not scattered cannot be detected by the CVFA receptors.

### *4.4. Modeling the retinal absorption and resulting scatter*

What is clear from the data above is that the spectral absorption profile of the blind hemiretina corresponds almost perfectly with the relative sensitivity reduction obtained for the blind hemifield when compared to the good hemifield in our spectral sensitivity measurements. A question which may be raised is whether this selective absorption of light in the blind hemiretina of our hemidecorticated patients corresponds to a specific absorption profile obtained in these patients. We believe that there is no obvious reason why the absorption profile for the blind hemiretina in these patients should be any different from that of a normal hemiretina. To

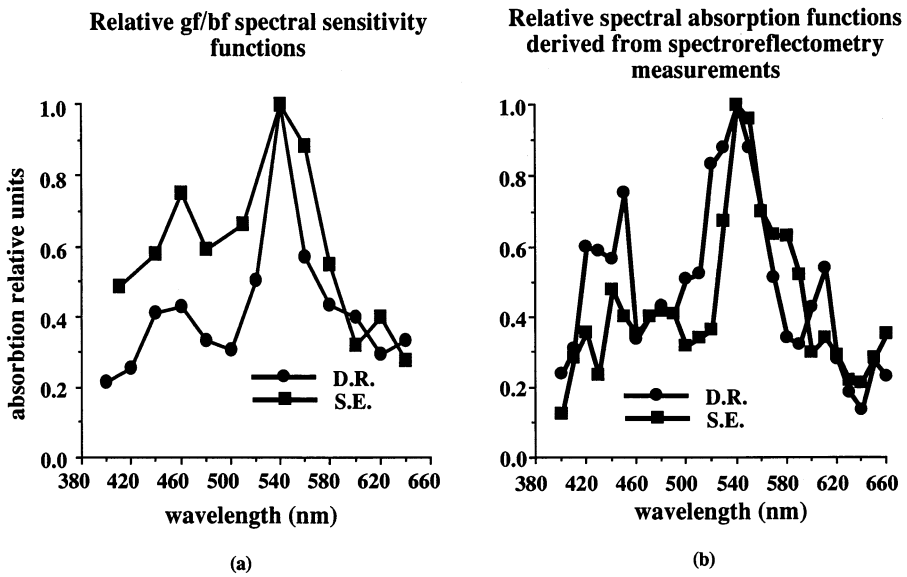


Fig. 5. Good/blind field sensitivity ratios for patients DR and SE (Fig. 5a). Note that there is a relative loss of sensitivity in the middle wavelengths of the visible spectrum in the blind field when compared to the good field. In vivo spectroreflectometry measurements made in the eyes of the same two patients are shown in Fig. 5b. These measurements are obtained by establishing the relative difference between the energy entering the eye and the energy coming out of the eye while taking into account the energy absorbed by the optics of the eyes.

illustrate our point we show in Fig. 6 a spetroreflectometry function for a normal observer obtained under identical conditions as those used to measure our patient data. The profile corresponds well to the absorption profile obtained for our patients' blind hemiretinas.

To demonstrate our point even further we have

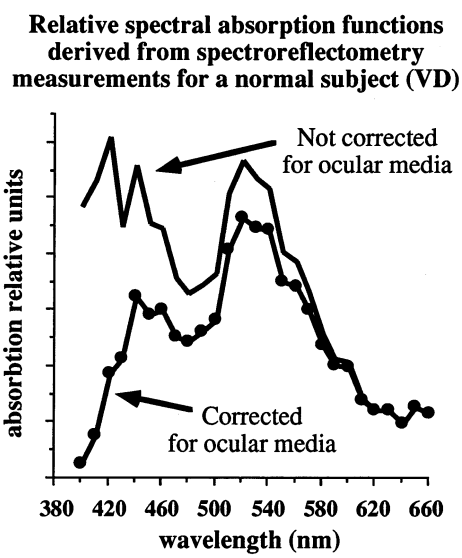


Fig. 6. In vivo spectroreflectometry measurements made in the eye of a normal observer obtained under the same conditions as the patient data shown in Fig. 5b. These measurements are obtained by establishing the relative difference between the energy entering the eye and the energy coming out of the eye while taking into account the energy absorbed by the optics of the eye. The solid curve shows the data when the ocular media is not accounted for and the line with round symbols shows the spectroreflectometry data when we correct for ocular media (see text and Appendix A for details).

quantitatively elaborated our reflective scatter model of residual vision by adapting to our specific conditions the van Nooren–Tiemeijer spectral reflectance and absorption model of the human eye (van Nooren & Tiemeijer, 1986). What is important to note is how the data represented in Fig. 5a (ratio between the good and bad field of the patients or the gf/bf ratio) and Fig. 5b (spectroreflectometry data) can be compared with one another (the mathematical details and derivations are presented in Appendix A). However, we can summarize and simplify the mathematical formulations by stating that we propose two ways of measuring the selective absorption of the retinal tissues which ultimately are represented as data in Fig. 5a,b. One method is by using the detection thresholds of the good and bad fields of our patients (Fig. 5a) and the other is by spectroreflectometry (Fig. 5b).

To compare the methods directly we must trace the light rays for the two types of 'reflectometry' measurements proposed above. In the first method we compare the detection thresholds in the good field with those of the bad field. In both the good and bad field data we can argue that the light travels through the ocular media for the entire length of the eye only before it reaches the detectors. In this case the ocular media factor can be simplified out of the gf/bf ratio and there is no need to correct for ocular media when comparing the results between the two fields. Essentially, it is argued that the light reaches the retina of the bad field, there is absorption by the retina, and then the light is redirected to the good field less some energy at specific wavelengths corresponding to the specific light components absorbed within the retinal layers.

In the second method we compare the light measured at the pupil entry with the light that exits the pupil. In this case the light rays reach the retina, some component is absorbed just like the gf/bf method mentioned above, and then the light is reflected back out of the eye. The difference in this case is that we must take into consideration the absorption of the ocular media twice for the reflected light because it travels the entire length of the eye going in and once again when it is reflected back out of the eye while the reference light (at pupil entry) never enters the eye and therefore is not affected by ocular media.

The derivations presented in Appendix A demonstrate that what we should be left with mathematically, using the model assumptions proposed above, is the retinal absorption when you factor out the ocular media. The actual data obtained with both methods presented in Fig. 5 corroborate the model results. The two curves shown in Fig. 6 represent the reflectometry measurements when the ocular media factor, as presented in Appendix A, is taken into account and when it is not taken into account.

## 5. Conclusion

In conclusion, we present a model to explain the potential effects of scatter properties of the eye on visual sensitivities obtained with hemidecorticated patients. The model clearly demonstrates that the sensitivity profiles obtained in the blind field of these patients may be derived from CVFA receptors. The model successfully demonstrates that intraocular Lambertian scatter off the back surface of the eye is probably the main source of the sensitivity obtained in the blind field of these patients when extraocular light scatter is controlled. Furthermore, the model predicts that it is theoretically possible to obtain very similar sensitivities from the normal and blind fields if large enough targets and/or eccentricities are used. We also demonstrate that the relative difference observed in the middle wavelength sensitivities between the good and blind hemifields of hemidecorticated patients is a result of selectively greater absorption of the eye for these wavelengths.

Although there might be a number of ways to control scatter we would suggest that a good method is to have a dynamic random luminance noise as a constant background for their stimulus display. This severely reduces any chance that the remaining functional areas of the visual field other than the testing site will respond to diffusion scatter. Local and global adaptation experiments such as those described in the present study would also prove useful to determine the actual response site for visual stimuli. Finally, intra- and extraocular scatter must be controlled in experiments that aim to show that there is light detection, whether conscious or unconscious, in the scotomata of cortically blind patients.

**Different components of the human eye included the absorption and reflection model**

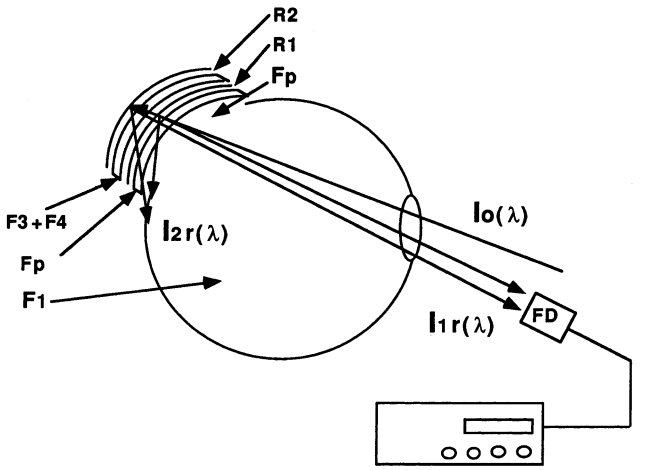


Fig. 7. Illustration of the eye and its different components which influence absorption and refelction of light in our model for residual vision. $F_1$ represents the ocular medium; $\alpha_1$ represents linear absorption coefficient of $F_1$; $d_1$ represents the thickness of $F_1$; $F_p$ represents the photopigment layer; $\alpha_p$ represents linear absorption coefficient of $F_p$; $d_p$ represents the thickness of $F_p$; $F_3$ represents the melanin pigment; $\alpha_3$ represents linear absorption coefficient of $F_3$; $d_3$ represents the thickness of $F_3$; $F_4$ represents the heamoglobin; $\alpha_4$ represents linear absorption coefficient of $F_4$; $d_4$ represents the thickness of $F_4$. $R_1$ represents the epithilium and $r_1$ corresponds to the reflection coefficient for $R_1$ $(0 < r_1 < 1)$; $R_2$ represents the sclera and $r_2$ corresponds to the reflection coefficient for $R_2$ $(0 < r_2 < 1)$.

## Acknowledgements

This project was supported by FCAR (Québec) and NSERC (Canada).

## Appendix A

The different retinal layers and the path of scattered light in the eye are represented in Fig. 7. The model can be quantitatively represented by the following formula (1):

$$I_1(\lambda) = I_0(\lambda) * 10^{-(2\alpha_1 d_1 + 2\alpha_p d_p)} * [r_1 + r_2(1 - r_1)^2 * 10^{-(2\alpha_3 d_3 + 2\alpha_4 d_4)}] * C(\Omega) \quad (1)$$

where $I_1(\lambda)$ represents the spectral luminance flux reflected by the pigment epithelium and the sclera at the level of the pupil exit, $I_0(\lambda)$ represents the initial spectral luminance flux, and $C(\Omega)$ is a constant which depends on the measurement geometry. For most of the reflection measurements obtained at the pupil exit we can assume that $C(\Omega)$ equals $10^{-3}$. We can simplify Eq. (1) by regrouping the coefficients corresponding to the retinal components and rewrite formula (1) as formula (1′):

$$I_1(\lambda) = I_0(\lambda) * 10^{-(2\alpha_1 d_1)} * 10^{-(2\alpha_P d_P)} *$$

$$[r_1 + r_2(1-r_1)^2 * 10^{-(2\alpha_3 d_3 + 2\alpha_4 d_4)}] * C(\Omega)$$

which can be simplified further into formula (1″);

$$I_1(\lambda) = I_0(\lambda) * 10^{-(2\alpha_1 d_1)} * r(\lambda)$$

where;

$$r(\lambda) = 10^{-(2\alpha_P d_P)} * [r_1 + r_2(1-r_1)^2 * 10^{-(2\alpha_3 d_3 + 2\alpha_4 d_4)}] * C(\Omega).$$

Simplified in this way, $r(\lambda)$ corresponds to a coefficient which is characteristic of the retinal reflection and absorption and $10^{-(2\alpha_1 d_1)}$ corresponds to the absorption within the ocular media.

If we apply these formulations to the specifics of our scatter-based model for residual vision in the blind field and our results shown in Fig. 5, we can say that we use two different procedures to measure the resulting reflection at the CVFA derived from scatter of a stimulus presented at 15° of eccentricity. One method (represented by the results in Fig. 5b) is to compare the luminance flux $I_0(\lambda)$ (which is our reference light) with $I_1(\lambda)$ (which is the light reflected by the back of the eye) as measured by a spetroradiometer. $I_0(\lambda)$ and $I_1(\lambda)$ are measured at the pupil entrance and at the pupil exit, respectively. Therefore the absorption is calculated as:

$$A_1(\lambda) = I_1(\lambda)/I_0(\lambda) = 10^{-(2\alpha_1 d_1)} * r(\lambda).$$

The second method (which corresponds to the data represented in Fig. 5a) is to measure the luminance flux $I'_0(\lambda)$ (the reference light) and $I'_1(\lambda)$ (the light reflected by the back of the eye) by using the CVFA detectors of the patient (as represented by our model in Fig. 1). In this case $I'_0(\lambda)$ represents the spectral sensitivity function obtained in the good field of the patient while $I'_1(\lambda)$ represents the spectral sensitivity function obtained in the bad field. As we have suggested previously, the model assumes that the detection of the stimulus presented in the bad field is in fact detected by the good field. It follows that the absorption in this case is represented as $A_2(\lambda) = I'_1(\lambda)/I'_0(\lambda)$ which should have the shape of $r(\lambda)$.

To be able to express $A_2(\lambda)$ and to compare it with $A_1(\lambda)$ it is necessary to first express $I'_0(\lambda)$ as a function of $I_0(\lambda)$, and $I'_1(\lambda)$ as a function of $I_1(\lambda)$. At the retinal level, the luminance flux $I'_0(\lambda)$ is represented as the luminance flux $I_0(\lambda)$ attenuated by the ocular media and measured as a spectral sensitivity function $F(\lambda)$ of the photoreceptors. Therefore:

$$I'_0(\lambda) = F(\lambda) * I_0(\lambda) * 10^{-\alpha_1 d_1}.$$

Similarly, $I'_1(\lambda)$ is represented as the luminance flux $I_1(\lambda)$ attenuated by the ocular media and measured as a spectral sensitivity function $F(\lambda)$ of the photoreceptors (Kitahara, Kandatsu, Tamaki & Matsuzaki, 1987).

It follows that:

$$I'_1(\lambda) = F(\lambda) * I_1(\lambda) * 10^{+\alpha_1 d_1} = F(\lambda) * I_0(\lambda) * 10^{-\alpha_1 d_1} * r(\lambda).$$

Therefore:

$$A_2(\lambda) = I'_1(\lambda)/I'_0(\lambda) = r(\lambda).$$

In this way it is possible to derive that the difference between $A_1(\lambda)$ and $A_2(\lambda)$ is the factor $10^{-(2\alpha_1 d_1)}$ which represents the ocular media. Fig. 6 shows the two spectroreflectometry functions when the ocular media is and is not accounted for.

## References


Campion, J., Latto, R., & Smith, Y. M. (1983). Is blindsight the effect of scattered light, spared cortex, and near-threshold vision? *The Behavioral and Brain Sciences*, *6*, 423–448.

Faubert, J., Diaconu, V., Ptito, M., & Ptito, A. (1995). Modeling visual scatter in the human eye: implications for residual vision. *Investigative Ophthalmology and Visual Science*, *36*, 633.

Fendrich, R., Wessinger, C. M., & Gazzaniga, M. S. (1992). Residual vision in a scotoma: implications for blindsight. *Science*, *258*, 1489–1491.

Hood, D. C., & Finkelstein, M. A. (1986). Chapter 5: sensitivity to light. In K. N. Boff, L. Kaufman, & J. P. Thomas, *Handbook of perception and human performance. sensory processes and perception*, Vol. 1. New York: Wiley.

King, S. M., Azzopardi, P., Cowey, A., Oxbury, J., & Oxbury, S. (1996). The role of light scatter in the residual visual sensitivity of patients with complete cerebral hemispherectomy. *Visual Neuroscience*, *13*, 1–13.

Kitahara, K., Kandatsu, A., Tamaki, R., & Matsuzaki, H. (1987). Spectral sensitivities on a white background as a function of retinal eccentricity. *Documenta Ophthalmologica Proceeding Series*, *49*, 651–655.

LeGrand, Y. (1958). *Light, Colour and Vision*. London: Chapman and Hall.

van Nooren, D., & Tiemeijer, L. F. (1986). Spectral reflectance of the human eye. *Vision Research*, *26*, 313–320.

Perenin, M. T. (1991). Discrimination of motion direction in perimetrically blind fields. *NeuroReport*, *2*, 397–400.

Perenin, M. T., & Jeannerod, M. (1978). Visual function within the hemianopic field following early cerebral hemidecortication in Man-I. Spatial localization. *Neuropsychologia*, *16*, 1–13.

Ptito, A., Lassonde, M., Leporé, F., & Ptito, M. (1987). Visual discrimination in hemispherectomized patients. *Neuropsychologia*, *25*, 869–879.

Ptito, A., Lepore, F., Ptito, M., & Lassonde, M. (1991). Target detection and movement discrimination in the blind field of hemispherectomized patients. *Brain*, *114*, 497–512.

Rushton, W. A. H. (1962). Visual Pigments in Man. *Scientific American*, *207*, 120–132.

Stoerig, P., & Cowey, A. (1995). Visual perception and phenomenal consciousness. *Behavioural Brain Research*, *71*, 147–156.

Stoerig, P., Faubert, J., Ptito, M., Diaconu, V., & Ptito, A. (1996). Blindsight in hemidecorticated patients? *NeuroReport*, *12*, 1990–1994.

Weiskrantz, L. (1986). *Blindsight: a case study and implications*. Oxford: Oxford University Press.

Wyszecki, G., & Stiles, W. S. (1982). *Color Science*. New York: Wiley.